Severe Weather

A SYNOPTIC ANALYSIS OF THE 6-7 MAY 1975 OMAHA TORNADO OUTBREAK

by James T. Moore (1)
and Harold A. Elkins (2)
Department of Earth and Atmospheric Sciences
Saint Louis University
St. Louis, Missouri 63103

ABSTRACT

The tornado outbreak of 6-7 May 1975, including the devastating Omaha, Nebraska tornado, is examined using surface, upper air and satellite imagery data. As early as 1200 GMT a narrow corridor of static and convective instability could be diagnosed over eastern Kansas, Nebraska and southern South Dakota underneath a 300 mb diffluent zone. Upper level positive vorticity advection and low level warm air advection helped to provide the lifting necessary to release this instability. Subjective analyses of pressure and dewpoint reveal that the squall line developed in the vicinity of a pressure trough located at the leading edge of a dry intrusion associated with a cold front. Objective analyses of temperature advection, moisture convergence and isallobaric divergence reveal these parameters' utility in the short-term forecasting of convection. Satellite imagery helps to show that the most severe activity took place near the intersection of a cold front and warm front where air in the warm sector was being lifted rapidly.

1. INTRODUCTION

During the 24 hour period from 1200 GMT 6 May to 1200 GMT 7 May 1975 at least 11 tornadoes and 15 severe thunderstorms developed within a corridor extending from southeast South Dakota to central Missouri (Figure 1). This devastating convective outbreak included at least three tornadoes, namely the Magnet, Hoskins and Omaha, Nebraska tornadoes, which were of F3 or greater intensity (3). Magnet and Hoskins are located to the north and northeast of Norfolk, Nebraska (OFK), respectively. The Magnet tornado (F4) touched down just before 2000 GMT, 6 May destroying most of the town before lifting. Shortly thereafter, a F3 tornado formed and descended 4 miles east of Hoskins causing damage to farms, livestock and power lines. At 2133 GMT the Omaha tornado (F4) touched down just south of Omaha and swept through the city, miraculously killing only 3 people while injuring at least 133 more (4).

There are several unique aspects to this severe weather outbreak that make it worthy of closer inspection. First, as noted by Miller (5), the squall line responsible for this severe weather developed along the leading edge of a pronounced dry intrusion. This dry intrusion, however, was associated with an occluding cyclone and was characterized by a moderate thermal gradient as well. It has characteristics similar in some ways to the "classic" dryline definition proposed by Schaefer (6) and applied to the Texas/Oklahoma dryline. Rhea (7) has shown that this dryline boundary is a "highly preferred thunderstorm developmental zone". Thus, regardless of its origin or the presence or absence of a thermal gradient, the dry intrusion plays a significant role in the genesis of convection.

Secondly, the Omaha outbreak demonstrates the importance of the intersection of surface boundaries in enhancing and localizing moisture convergence. This has been graphically shown by Purdom (8) and others to be an important physical process that can be vividly captured by satellite imagery. In the discussion that follows it will be shown that although the squall line developed along the leading edge of the dry intrusion, the most severe convection took place in the vicinity of the developing occlusion. Apparently, the warm moist air in the warm sector was lifted more rapidly near the occlusion, allowing for the quick release of conditional and convective instability. Thus, there was a continual development of the most intense convection from the northwest to the southeast, following the point of the occlusion.

This synoptic study was prompted by the desire to investigate those physical processes contributing to this narrow outbreak of severe convection. The 125 km - 1 hour space-time resolution of the surface network and the 400 km - 12 hour space-time resolution of the convectional upper air network are utilized to examine the key hydro- and thermodynamical parameters active both prior to and during the severe outbreak. At the surface subjective analyses of surface pressure and dewpoint will be shown to document the position of the dry intrusion, troughs and wind shift lines. Mesoanalysis of surface variables has been documented by Whiting (9) and Miller (10) among others, to be useful in diagnosing the potential for severe convection. Kuhn et al. (11) and Karkow et al. (12) have

shown that tornadoes tend to develop along and to the east of surface thermal ridges which are oriented parallel to the gradient flow. More recently, Moller (13) has shown that the AVE-SESAME I tornado outbreak preferentially took place between the surface thermal and dewpoint ridges, with the optimum position of the thermal ridge being to the west of the dewpoint ridge.

In addition, objective analyses of surface moisture convergence, thermal advection and isallobaric convergence are displayed to demonstrate the utility of these parameters in isolating the severe weather threat area. Several researchers (14, 15, 16, 17) have documented the effective use of moisture convergence as a short-term predictor of severe convection, especially when it is strong and demonstrates good space-time continuity. Warm air advection at the surface associated with the development of a thermal ridge will lead to stability decreases with time. In the vicinity of a frontal boundary warm air advection will also be indicative of isentropic upslope flow which may release potential instability (16). Finally, convergence due to a concentrated region of pressure rises/falls (isallobaric convergence) has often been cited as a useful parameter to diagnose future convective areas. Moore and Fuelberg (18) diagnosed strong pressure falls approaching -7 mb/3 hour which preceeded the severe convection that took place during the AVE-SESAME I outbreak. Low level convergence, enhanced by the ageostrophic flow induced by the isallobaric wind, can often help to erode the inversion or "lid" which is restricting convection (19). Once again, the space-time continuity of the isallobaric convergence field is important when used as a short term severe convection parameter.

The precursor upper air conditions for 1200 GMT, 6 May are examined, as well for 850, 700, 500 and 300 mb. These charts are subjectively analyzed to document differential thermal/moisture advection, jet streak positions, diffluence and the presence of short wave troughs in the same manner discussed by Miller (10) and Doswsell (16). Objective analyses of the relative vorticity at 500 mb and divergence at 300 mb help to diagnose mid-level short waves and the presence of strong upper level divergence, respectively. The influence of upper level jet structure on the divergence profile has been noted by Beebe and Bates (20), House (21) and, more recently, McNulty (22). Many times a favorable environment for the release of potential in stability can be found in the upper air dynamics of jet streaks, especially in baroclinic outbreaks associated with cyclogenesis.

Thus, we hope to shed light on the following questions concerning this severe weather outbreak:

1) Why was the convection restricted to such a relatively narrow area?

2) What upper air features on the morning of 6 May helped to support the severe storm environment?

3) What surface parameters could have been utilized to help isolate the watch areas in both space and time?

4) How may satellite imagery have been used to further diagnose the greatest threat area within the severe storm environment?

2. DATA AND ANALYTICAL PROCEDURES

Hourly surface data for 6-7 May 1975 from first order stations in the states of South Dakota, Nebraska, Kansas, Missouri, Iowa and Minnesota were obtained from the National Climatic Data Center in Asheville, North Carolina. The same facility also supplied rawinsonde data for 1200 GMT 6 May and 0000 GMT 7 May 1975 for most of the upper air stations north of 35°N latitude and from 35°-110°W longitude. Visible satellite imagery was made available from the National Environmental Satellite, Data and Information Service (NESDIS). Finally, National Weather Service (NWS) radar summaries were taken from the National Facsimile Circuit (NAFAX).

Nearly 80 surface stations were used to interpolate data onto a 14 x 13 grid approximately centered on Omaha, Nebraska (OMA). The domain of this grid is shown in Figure 2. The grid interval was 95.25 km on a polar stereographic projection, true at 60°N. A Barnes (23) objective analysis routine was utilized to interpolate the station data to the grid points. A scan radius of 333 km was used, together with four iterations to yield the response curve shown in Figure 3. As the latter diagram shows, this combination of objective analysis parameters permitted greater than 95% resolution of the amplitude of those wavelengths greater than 600 km and less than 63% resolution of the amplitude of those wavelengths less than 400 km. Since the average station spacing was about 125 km, the minimum resolvable wavelength was 250 km (a 2Δ wave). The Barnes scheme has implicitly, through its weighting function, damped those wavelengths less than 250 km, as seen in Figure 3. However, it can be safely stated that the conventional surface network is capable of resolving meso alpha scale (24) waves, which typically play important roles in organizing and initiating convection. Temperature advection, moisture convergence and the divergence of the isallobaric wind were computed from the objective analyses of wind (u and v components), mixing ratio, temperature and pressure tendencies. All of these fields were computed using second order, centered finite differences. The pressure tendencies used in computing the isallobaric wind and its

divergence were based on 3 hour pressure changes.

Subjective analyses of the sea level pressure and surface dewpoints are also shown in Section 3. These fields were not objectively analyzed for fear of losing the detail in the small scale waves present in the pressure and dewpoint pattern. Doswell (16) notes that surface subjective analysis can be critical in diagnosing subtle features often "overlooked" or smoothed out by objective analysis schemes. Examples of this will be seen in Section 3 (see Figure 14a, for example) when the surface dewpoint field display small scale "bulges". These subject surface analyses were scrutinized to check for spatial and temporal continuity of key features to assure that the authors were not analyzing spurious noise in the data.

Twenty-two rawinsonde stations were used in the upper air grid shown in Figure 4. This 21 x 19 grid utilized the same map projection and grid interval as the surface scheme. Due to the increased station spacing (apporximately 400 km), a scan radius of 619 km was used, together with 4 iterations of the Barnes scheme to objectively interpolate data to grid points. The response function for this objective analysis is shown in Figure 5. As can be seen, greater than 60% of the amplitude of those wavelengths greater than 1000 km was resolved, while only 25% of the amplitude of the minimum resolvable wavelength of 800 km was resolved. Thus, as expected, the upper air network was capable of resolving macro beta (synoptic scale) wavelengths with some resolution of those waves belonging to the meso alpha scale. Therefore, at best, the conventional upper air network allows one to capture those synoptic scale features which act to support or enhance the severe storm environment. The objective analyses of u and v wind components were utilized to compute the relative vorticity at 500 mb and divergence at 300 mb. Once again, derivatives were computed using second order, centered finite differences.

Lifted indices were computed directly from the rawinsonde data in order to assess the stability. The mean mixing ratio and potential temperature of the lower 100 mb of the sounding were utilized to define a boundary layer lifting condensation level (LCL). From the LCL the parcel was lifted pseudo-adiabatically to 500 mb. The Lifted Index was computed by subtracting the parcel temperature at 500 mb from the environmental temperature at the same level.

Finally, subjective analyses of the 850, 700, 500 and 300 mb pressure surfaces are shown to emphasize the position of short wave troughs, dry and moist tongues and the presence of jet streaks.

3. RESULTS

In this section we shall first explore the initial surface and upper air conditions at 1200 GMT, 6 May through both subjective and objective analyses. The Omaha, Nebraska sounding will also be examined to diagnose the degree of instability, depth of the moist layer and vertical wind profile. Then, following in the steps of a severe storm forecaster, we will document the changes in key surface parameters that led up to the convective outbreak.

3.1 INITIAL CONDITIONS

Figure 6a displays the surface conditions at 1200 GMT, 6 May 1975 over the upper Midwest. A closed surface low with a central pressure of 991 mb is situated in southwest South Dakota. From this low a cold front protrudes to the southeast towards central Kansas. This cold front lies along the leading edge of a remarkably strong dewpoint gradient, normally associated with dry lines (6). Dewpoints are around 65°F (18.3°C) in eastern portions of Kansas and Nebraska but are less than 20°F (-6.7°C) in western portions of Kansas. This feature cannot rigorously be called a dryline since it is also accompanied by a significant temperature gradient and will be referred to as a dry intrusion. Temperatures decrease from greater than 65°F (18.3°C) in eastern Kansas and Nebraska to near 40°F (4.4°C) in western regions of those states. The plotted data also reveal a well-defined wind shift from southeasterly (approximately 160°) to southwesterly (approximately 230°) across the cold front. Thus, although this feature is not a true dryline, it has many similarties to the classic Texas/ Oklahoma dryline representing the leading edge of dry, westerly momentum. It is not immediately apparent whether this dry air is due to horizontal advective processes from the southwest United States (19) or from subsidence as air descends on the lee side of the Rockies (6, 25).

The moist air is defined as a narrow tongue, coincident with the thermal ridge (not shown) from eastern Kansas to southern South Dakota. Temperatures and dewpoints decrease once again to the northeast over Missouri, Iowa and eastern South Dakota, where winds become decidedly more easterly. This suggests the presence of a warm frontal boundary along the southern edge of the dewpoint/thermal gradient. The National Meteorological Center (NMC) surface analysis did diagnose a warm front in this area. Miller (5) notes that the air in northwest Missouri and extreme eastern Nebraska was rain-cooled by previous thunderstorm activity. The latter author maintains that this surface boundary was actually created by thunderstorm outflow. It could be that a pre-existing weak frontal boundary was actually enhanced by the cool thunderstorm outflow. Lack of earlier data prevents a

more definitive conclusion concerning the origin of this boundary.

The moisture convergence field shown in Figure 6b for the same time reveals a positive axis from a position near the low pressure center to southeastern Nebraska south to central Kansas. Experience with this parameter (17) suggests that space-time consistency is just as important as the magnitude in judging its relative importance in the severe storm environment. Interestingly, the temperature advection field shown in Figure 6c reveals that a warm advection axis is superimposed over the moisture convergence axis. Thus, this region is experiencing warm, moist air advection and is subject to convergence as well. So, as early as 1200 GMT the low level severe storm environment is being created.

The 850 mb chart shown in Figure 7a reveals a thermal ridge extending from eastern Oklahoma northward to eastern South Dakota. This is coincident with a narrow tongue of high relative humidity, indicated in Figure 7a by a stippled region of dewpoint depressions less than or equal to 5^{o}C. Although the 850 mb surface is below ground to the west it is possible to diagnose a wind shift line, indicative of a trough, from the low center over the Nebraska panhandle southward through central Kansas and western Oklahoma.

At 700 mb (Figure 7b) a low center is found over eastern Wyoming with a trough axis extending southeastward to the Texas Panhandle. Comparison of the position of the trough axes at the surface, 850 and 700 mb reveals the westward tilt of this system, attesting to its baroclinicity. Importantly, the isotherm analysis indicates a warm tongue over the same region described on the 850 mb chart. However, an examination of the dewpoint depression reveals very dry air (dewpoint depressions greater than 20^{o}C) extending east-northeast from eastern Nebraska and Kansas, over Iowa and northern Missouri, to central Wisconsin. Superimposing this dry air at 700 mb over the moist tongue at 850 mb (Figure 7a) helps define a region of convective instability. Figure 7c further defines the area of convective instability as it displays a field of the maximum, continuous, vertical decrease in the equivalent potential temperature (theta-e) computed from sounding data. This field reveals a region where theta-e decreases more than 20 K running south from eastern South Datoka to eastern Kansas and east to central Iowa and northern Missouri. Note especially the 30 K decrease in theta-e over Omaha. It should be pointed out that most of the theta-e decreases greater than 20 K took place over a layer approximately 50-150 mb deep. In the standard atmosphere the maximum negative change in theta-e is about -5.5 K over a 300 mb layer. Thus, the convective instability shown in Figure 7c is about 5 to 6 times greater than in the standard atmosphere.

At 500 mb (Figure 7d) a low center of 5440 gpm is located over southern Wyoming. A jet streak with a 37 m/s core is seen on the eastern side of the closed low moving into western Nebraska. It is important to point out that the subsequent severe convective activity took place on the anticyclonic side and within the exit region of this jet streak. The relative vorticity field at 1200 GMT, displayed in Figure 7d, defines a short wave trough in Colorado. With a jet streak on the eastern side of the closed low, one would expect this trough and its relative vorticity maximum to "lift out" to the northeast. The movement of the short wave in this fashion would increase the positive vorticity advection (PVA) over Nebraska with time. Miller (10) has noted that 500 mb PVA is a key parameter for severe storm forecasting, useful in assessing the degree of upper level support for convection. It is important to note, however, that it is not just PVA at any one pressure level, but upward increasing PVA which is related to upward vertical motion. In addition, one must evaluate the thermal advection as well, in order to fully diagnose the sign of the vertical motion at any particular level (26).

At 300 mb (Figure 7f) maximum winds within the jet approach 45 m/s over northern New Mexico. On the anticyclonic side of the jet over northern Kansas and eastern Nebraska a strong diffluent zone is found. Evidence for this feature is shown in Figure 7g which displays the divergence at 300 mb at 1200 GMT. Note the protrusion of an axis of divergence coinciding with the diffluent zone from northwest Kansas to eastern Nebraska. This feature is significant since the sign of the divergence on the anticyclonic side of a cyclonically curved jet is qualitatively undefined (20). McNulty (22) emphasizes the need to determine the sign of the divergence at 300 mb in the vicinity of a wind maximum since his case studies reveal that "severe weather outbreaks occur under regions of upper divergence inferred from 300 mb wind maxima". As we see in this case it is not easy to infer the sign of the divergence from simple jet steak models especially in the case of a curved jet axis. A quatitative analysis of upper level divergence can be useful to the forecaster attempting to evaluate the severe storm scenario.

An examination of the stability at 1200 GMT, through the lifted index (LI) field (Figure 8) reveals a narrow tongue of LI's less than zero which broadens to the southeast. Omaha, Nebraska's (OMA) value of -4.0 represents a minimum for this field. Strong stability (LI's greater than 14) is found to be southwest and northeast of OMA. Figure 9, which shows Omaha's sounding at this time, illustrates several key points concerning stability and the

supporting vertical wind shear. Specifically one finds the following:

1) a moist low level layer of about 185 mb depth.

2) a deep, dry middle layer from about 785-535 mb which, together with 1) created a convectively unstable column,

3) a strong inversion from 787-760 mb over which the temperature increases 6.2°C, acting as a strong inhibitor of convection, and

4) considerable veering of the wind with height mostly in middle levels with speed shear concentrated mostly below 500 mb.

Soundings for Rapid City, South Dakota (RAP) and Topeka, Kansas (TOP) were analyzed, too. At RAP (not shown) there was dry air aloft over moist, low level, air. However, surface temperatures were about 50°F, substantially cooler than at OMA. Also, although an inversion was diagnosed at 700 mb, it was far weaker (approximately isothermal) than the OMA inversion depicted in Figure 9. The TOP sounding (not shown) was similar to the OMA sounding, except for the presence of a weaker inversion and weaker vertical wind shear. Thus, the initial "ingredients" for severe weather were present. The forecaster's job from here on was to search the future surface observations and satellite imagery for those short-term features/parameters which would indicate when and where this convective potential would be released.

3.2 CONDITIONS LEADING UP TO THE OUTBREAK

Surface pressures and dewpoints at 1500 GMT, shown in Figure 10a, reveal that the cold front/dry intrusion identified earlier in Figure 6a has moved slowly eastward. The leading edge of this feature generally parallels the 60°F (15.6°C) isodrosotherm. The wind shift associated with the front is one of southeasterly momentum preceeding it to southwesterly momentum behind it. A second, more subtle wind shift and dewpoint gradient is observed across the warm frontal boundary. This front is not only associated with a dewpoint gradient but cooler temperatures and easterly momentum to the north and warm, moist southerly momentum to the south. Note how, as the occlusion process takes place, the warm sector becomes more narrow as the warm, moist air is lifted. However, satellite imagery revealed little or no activity in this area at this time.

The surface moisture convergence field at 1500 GMT (Figure 10b) continues to reveal an organized positive axis from southwest South Dakota to eastern Nebraska which then branches into northern Missouri and eastern Kansas. The surface thermal advection field shown in Figure 10c also reveals a warm advection axis with the same northwest-southeast orientation. Importantly, values have increased over eastern Nebraska to over 0.6 K/hour. Although the moisture convergence and warm advection magnitudes over Nebraska are less in magnitude than those found in eastern Kansas, they do display greater space-time continuity over the last three hours. In addition, the south central Kansas maximum is located near the border of the grid which may lead one to suspect that it is a result of the objective analysis scheme, rather than the data. Thus, although one would not disregard the latter maximum in Kansas, one would place less emphasis on it at this time.

Another parameter, less frequently cited as a useful severe storm parameter, is isallobaric divergence. Since the surface pressure is affected by the integrated divergence and density advection in the column, pressure tendencies are direct indicators of changes aloft. In this case we have computed the isallobaric divergence from the isallobaric wind, itself obtained from a 3 hour pressure tendency field (e.g., 1200-1500 GMT). Again, experience has shown it to be a useful, short-term predictor of severe convection when it displays good space-time continuity. One can think of isallobaric divergence (convergence) as a potential divergence (convergence), realized only when the real wind is turned sufficiently by pressure rises (falls) to enhance/destroy the in situ divergence field after several hours.

The 1200-1500 GMT isallobaric divergence field shown in Figure 10d shows isallobaric convergence over the same region shown in Figures 10b and 10c to be experiencing moisture convergence and warm air advection. Values exceeding -8×10^{-5} s^{-1} are found throughout the well-defined corridor, which includes eastern Nebraska and eastern Kansas. The coincidence of instability, warm air advection, moisture convergence and isallobaric convergence define the future convective line. The timing of the formation of individual supercells is below the resolution of these data sets. However, the merger region of the thermal/moisture boundaries seems to be an area worth watching. Satellite imagery, along with radar, are useful in further pinpointing what restricted regions within the corridor may convectively erupt.

Surface pressure and dewpoints at 1800 GMT (Figure 11a) reveal the slow movement of the cold front/dry intrusion eastward. The dewpoint analysis shows that the dry air protrusion to the east is anything but uniform. There appear to be several "bulges" along the dry intrusion, indicative of the fact that vertical mixing often is enhanced more in one area than another. This is due to local

stability profiles, which often create bulges; many of these produce regions of enhanced convection downstream (27).

Importantly, the intersection between the cold front (now a developing squall line) and the weak warm frontal boundary appears to be in northern Nebraska. These boundaries are corroborated by satellite imagery shown in Figure 12. Satellite imagery reveals a squall line coincident with the cold frontal boundary, and a "shear line", which has been identified in this paper as a warm front. The latter is especially identifiable by the change in cloud type from stratiform (cold side) to cumuliform (warm sector) clouds. Note that where these two boundaries intersect a strong cell developed, within which the Magnet, Nebraska tornado formed at about 2000 GMT.

The moisture convergence field at 1800 GMT (Figure 11b) continues to show a northwest-southeast positive axis with a maximum value of 4.0 gm/kg-h over south-central South Dakota. Values greater than 2.0 gm/kg-h persist over eastern Nebraska and Missouri. Simlarly, the thermal advection field at 1800 GMT (Figure 11c) continues to reveal moderate warm air advection over this corridor. Note how the secondary maximum in moisture convergence and thermal advection over Nebraska closely correlate with the position of the intersection of the two thermal boundaries noted earlier. Values of moisture convergence and warm air advection are strong in western South Dakota as well. The isallobaric divergence field (Figure 11d), based on pressure tendencies from 1500-1800 GMT, continues to show strong isallobaric convergence on a northwest to southeast line over the corridor. This would indicate continued enhancement of low level convergence in Nebraska and Missouri. One would expect the strongest development in the vicinity of the boundary intersection which is moving southeastward within the corridor of instability.

Figure 13 displays a National Weather Service radar summary for 1935 GMT. This is about 1 1/2 hours after the last map series. Notice that the strongest cells are in eastern portions of Nebraska and Kansas. At this time the boundary intersection point was approximately located just northeast of Norfolk, Nebraska (OFK on surface maps). Thus, the air to the south of the intersection point is being lifted as it gets "squeezed" between the advancing cold front and the slowly moving warm front.

The last series of maps shows conditions 33 minutes before the Omaha tornado touched down south of the city. At 2100 GMT the leading edge of the dry intrusion is located in southeastern South Dakota, along the Nebraska/Iowa border into eastern Kansas (Figure 14a). As noted in Figure 12 in the satellite imagery, the cold front at 2100 GMT intersects the warm frontal boundary at a position just west of Omaha, Nebraska. An active cell grew quickly in this vicinity and spawned the F4 Omaha tornado.

Figure 14b shows the moisture convergence field at 2100 GMT. Two maxima are located within the severe convective corridor, one in south-central South Dakota, and the other in extreme northwestern Missouri. Tracking the latter maxima reveals that it moved southeastward over the last three hours, nearly coincident with the boundary intersection point. At 2000 GMT (not shown) there was a 2.3 gm/kg-h maxima just west of Omaha; this shows the utility of moisture convergence fields in the 1 to 3 hour time frame for predictive purposes. The northern maxima was accompanied by convection as well, but of lesser intensity. The severity of the southern convection was apparently due to (1) the strength of the inversion over Nebraska and its role in restraining convection until the time of maximum heating, (2) the degree of convective instability, (3) proximity to the thermal/moisture boundary intersection, and (4) the structure of the vertical wind shear.

The thermal advection pattern at 2100 GMT (Figure 14c) reveals strong warming in the vicinity of Omaha, with values around 0.6 K h^{-1}. This parameter, together with moisture convergence, has helped in objectively following the intersection point as it traveled southeastward over the last six hours.

Finally, the isallobaric divergence field shown in Figure 14d diagnoses two minimums, one near Omaha and another in southeastern South Dakota. A major part of this isallobaric convergence is due to a pressure fall of 3.1 mb associated with a heavy thunderstorm that Omaha experienced prior to the tornado. Undoubtedly, this helped to enhance low level convergence on an even smaller scale than can be diagnosed through surface data. This may have been a catalyst for tornado genesis.

In later time periods the intersection point of the two boundaries moved east- southeast. Subsequent severe convection developed in Iowa and Missouri, weakening as the night progressed. In Missouri most of the activity was in the form of severe thunderstorms, some with hail.

4. CONCLUSIONS

We have sought to depict those atmosheric processes responsible for the convective outbreak of 6-7 May 1975, culminating in the Omaha, Nebraska tornado. Importantly, we have tried to follow the chain of events as they might have been watched by a severe storm forecaster on that day, had various key parameters been available to him/her in realtime. Towards this end it has been shown that:

1) the convection broke out ahead of a cold frontal boundary which was also the leading edge of southwesterly momentum and a strong dewpoint gradient.

2) a narrow tongue of strong static and convective instability could be diagnosed as early as 1200 GMT, 6 May over eastern Kansas, Nebraska and northern Missouri due to moist, low level air being capped by warm, dry, middle level air.

3) surface heating and moisture convergence acted to increase the instability with time over a narrow corridor which included eastern Nebraska. Moisture convergence and isallobaric convergence, overlain by 300 mb divergence, helped to generate the lifting needed to release the instability in this region.

4) the strongest convection took place in the vicinity of the "triple point" of an occluding cyclone as air in the warm sector was lifted; satellite imagery helped to document this frontal boundary intersection point, and

5) surface objective analyses of moisture convergence, temperature advection and isallobaric divergence helped to diagnose and forecast the squall line and its more intense regions.

Thus, this severe outbreak was restricted to a relatively narrow area due to several factors. First, the region of convective and static instability (see Figures 7c and 9, respectively) were well-defined between a cold front/dry intrusion boundary and a warm frontal boundary. Secondly, the area of greatest vertical lifting was within the warm sector which likewise was a relatively confined region. Finally, the surface parameters presented showed that low level forcing of moisture convergence, warm air advection and the convergence of the isallobaric wind was restricted to a northwest-southeast corridor. So, both the instability and the mechanisms forcing its release helped to define a specific volume of the atmosphere as a severe convective zone.

Overall, this study emphasized the utility of surface data and objective analysis of key surface parameters in anticipating the development of deep convection. It is important, as well, to get a good picture of the initial upper air forcing in order to see if there are any significant features aloft which would either help or limit the degree of convection. Satellite imagery proved to be useful in diagnosing the presence of two convergence lines or boundaries. At their intersection (the occlusion) a "hot spot" for convection produced an environment favorable for tornadogenesis.

Once again it is proven that one needs a good diagnostic picture of the atmosphere before one attempts to forecast.

ACKNOWLEDGEMENTS

The authors would like to thank Mr. James Purdom of NESDIS for supplying us with the satellite imagery and analysis in Figure 12. His experience with this storm case also helped guide the writing of this paper. We also thank Mr. John Weaver and Mr. Ray Zehr of NESDIS for their helpful criticisms of a preliminary draft of this paper. Mr. Jon Chrzanowski is appreciated for his help in drafting many of the diagrams. We also thank our friends, Dr. John Zack, Mr. Ronald Przybylinski, and Mr. William Sammler, who reviewed the early stages of this paper. The anonymous reviewer of this paper is sincerely thanked for his/her useful comments in the preparation of the final version of this paper. Much of this work stems from the principal author's Ph.D. dissertation, completed while at Cornell University. Ms. Rhonda Webb is appreciated for her work in masterfully preparing the manuscript.

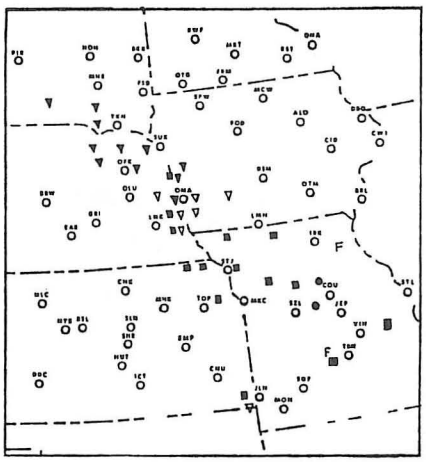

Figure 1. Severe weather events observed between 1200 GMT 6 May and 1200 GMT 7 May 1975. Solid triangles are tornadoes, open triangles are funnel clouds, solid squares denote severe thunderstorms with hail, while solid circles indicate severe thunderstorms.

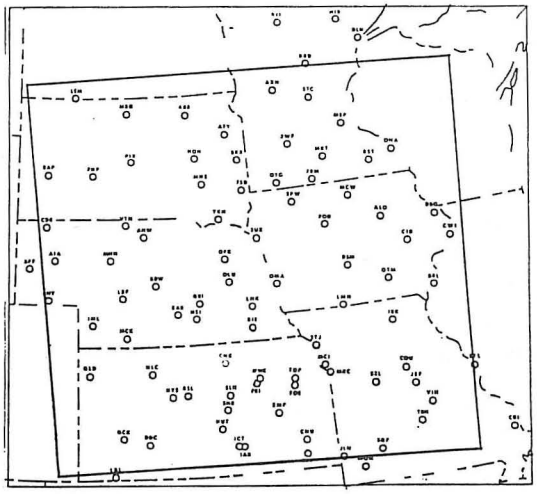

Figure 2. Surface stations utilized for subjective and objective analyses. The inset rectangular region is the domain of the grid used in the objective calculations.

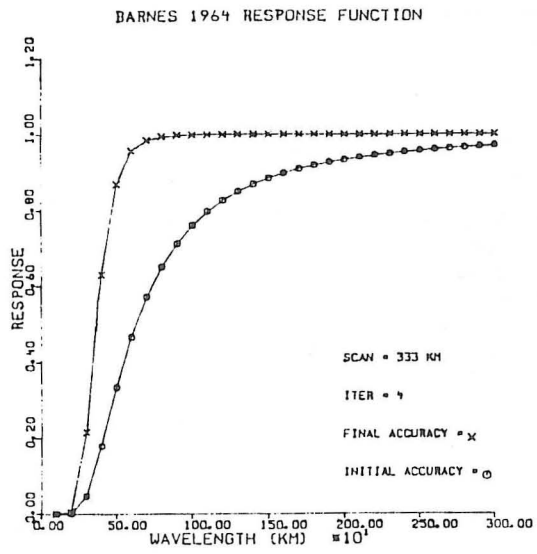

Figure 3. Barnes (23) response function for surface objective analyses. Each plotted point is at a 100 km increment.

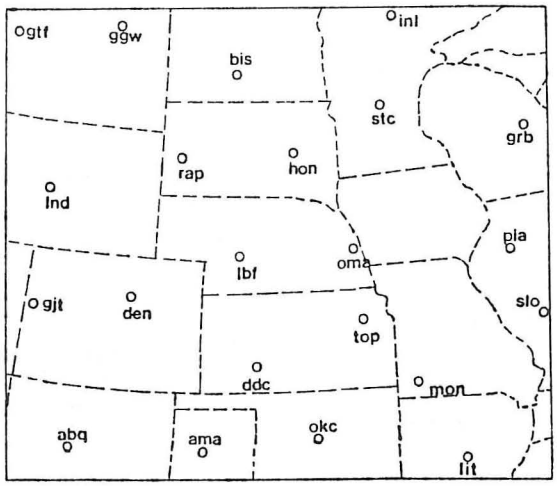

Figure 4. Upper air stations utilized for subjective and objective analyses.

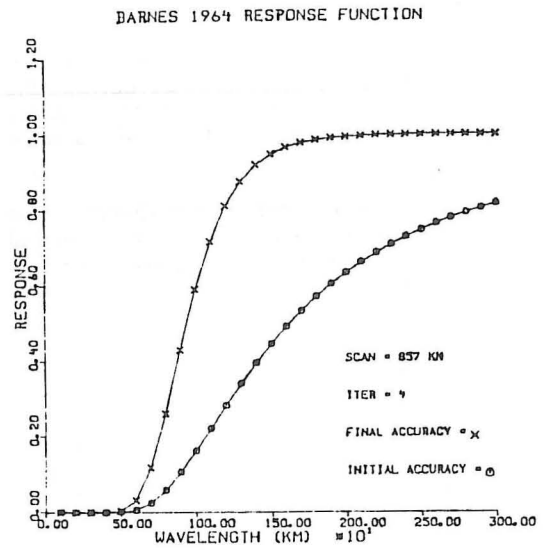

Figure 5. Barnes (23) response function for upper air objective analyses.

If you have enjoyed reading this issue of the National Weather Digest, please pass it on to a friend when you are through. Thank you!

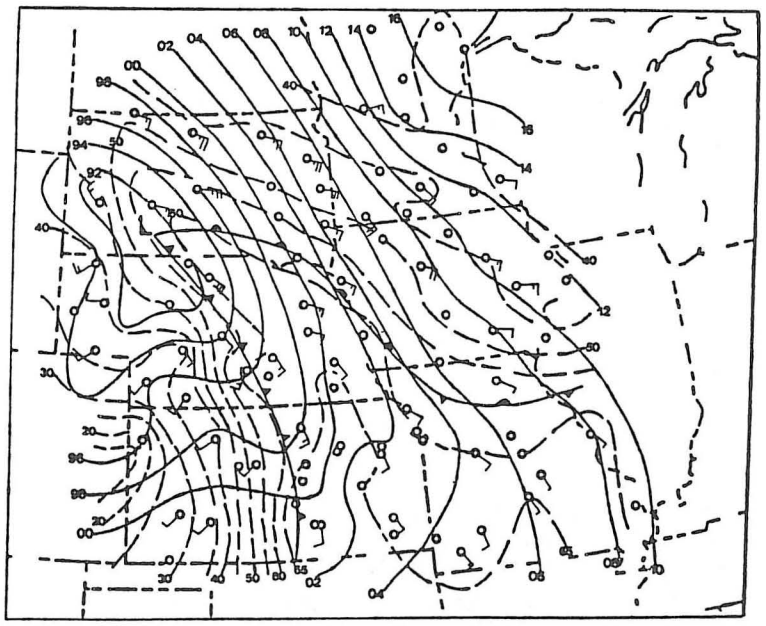

Figue 6a. Surface conditions for 1200 GMT, 6 May 1975. Solid lines are isobars in mb where the preceeding 9 or 10 has been omitted. Dashed lines are isodrosotherms in °F. (Subjective analysis).

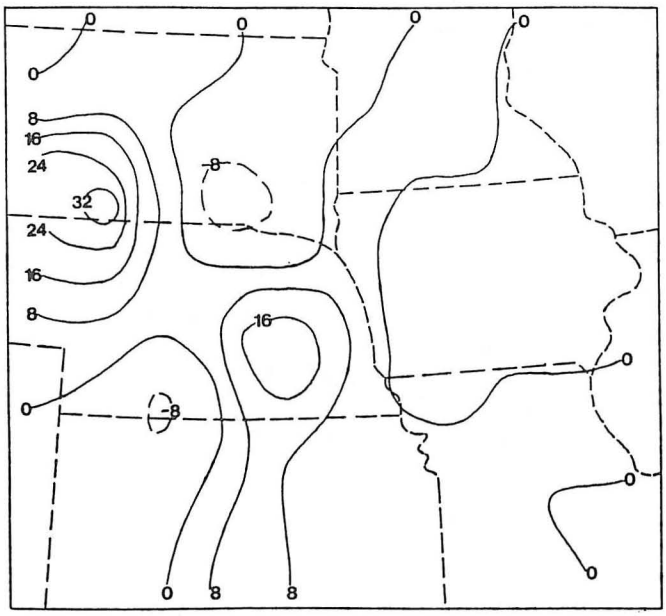

Figure 6b. Surface moisture convergence for 1200 GMT, 6 May 1975. Values are x 10 gm/kg-h (e.g., 16 = 1.6 gm/kg-h). Positive values indicate moisture convergence.

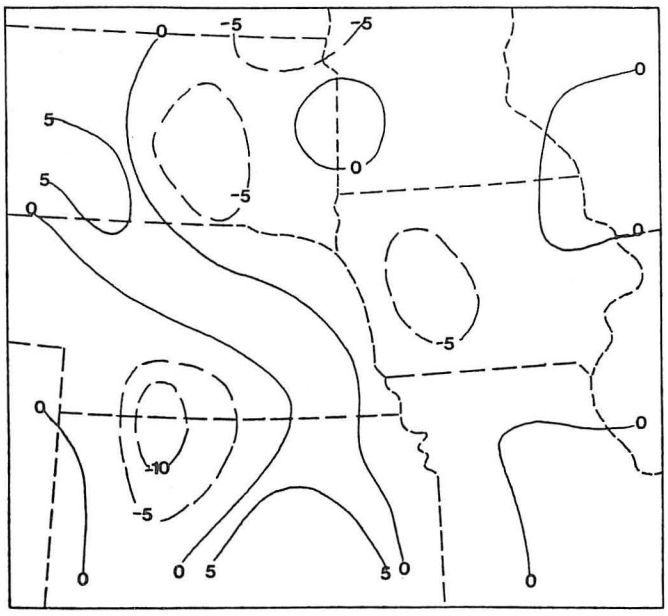

Figure 6c. Surface temperature advection for 1200 GMT, 6 May 1975. Values are x 10 K/h (e.g., 5 = .5 K/h).

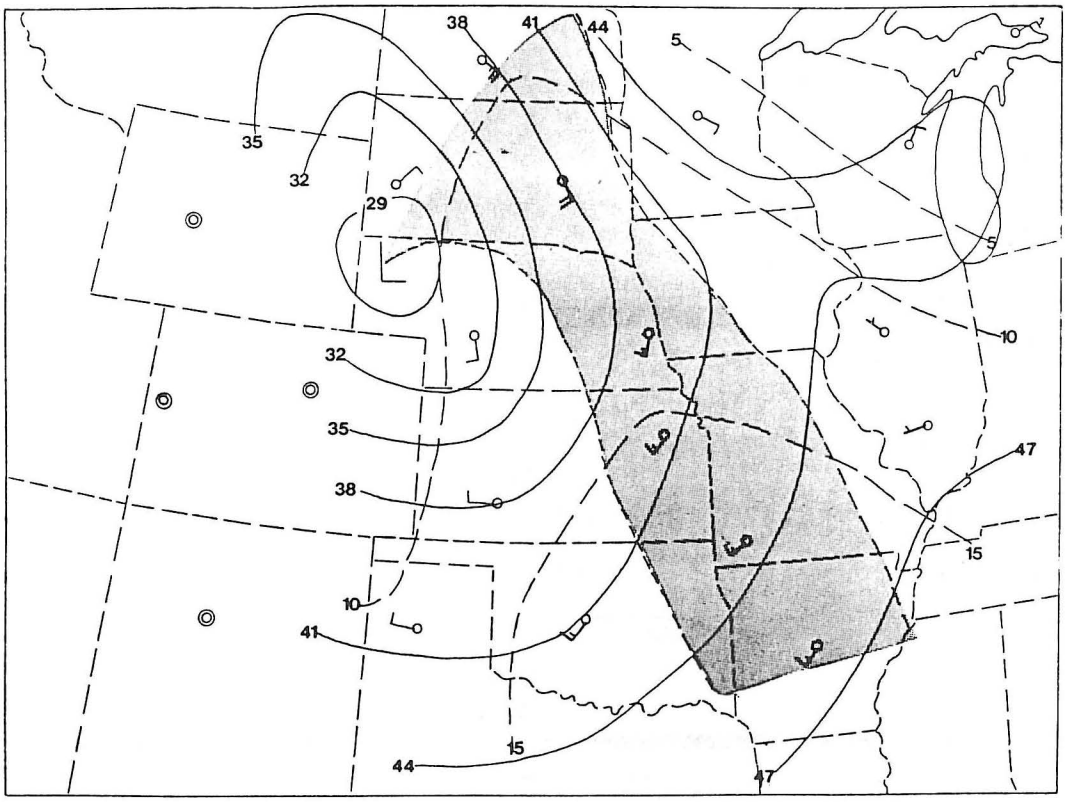

Figure 7a. 850 mb chart for 1200 GMT, 6 May 1975. Solid lines are heights in decameters where the preceeding 1 has been omitted. Dashed lines are isotherms in °C. Stippled area indicates dewpoint depression less than 5 °C. Plotted winds as m/s.

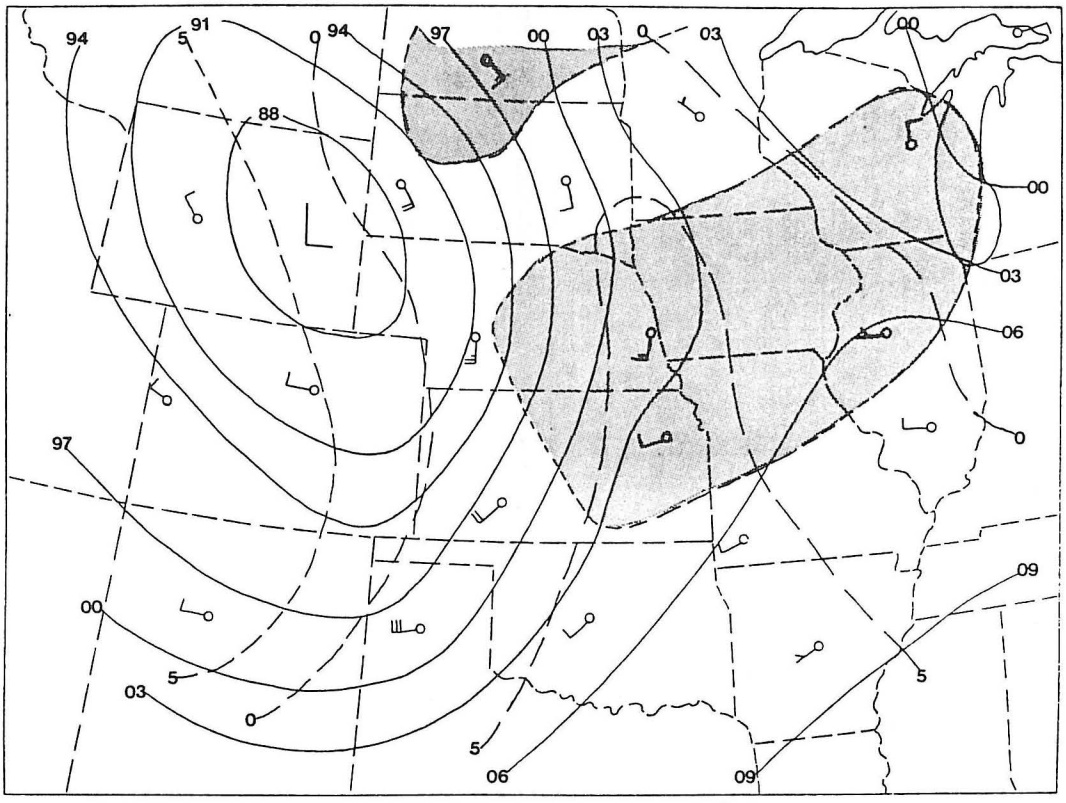

Figure 7b. 700 mb chart for 1200 GMT, 6 May 1975. Solid lines are heights in decameters where the preceeding 2 or 3 has been omitted. Dashed lines are isotherms in °C. Stippled area indicates dewpoint depressions greater than 20°C. Plotted winds are in m/s.

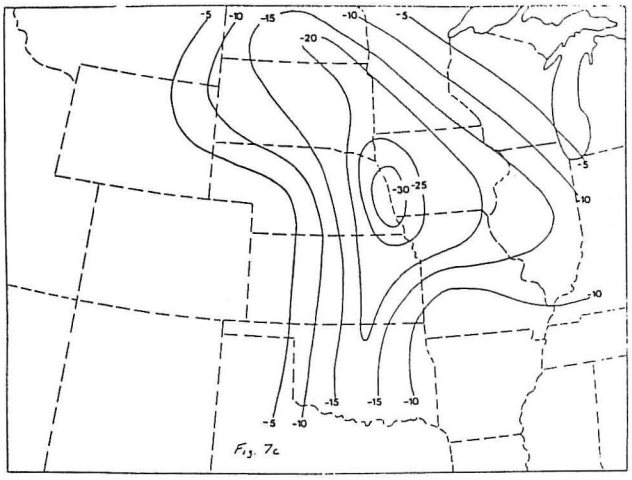

Figure 7c. Maximum, continuous decrease in the equivalent potential temperature (theta-e) in K for 1200 GMT, 6 May 1975. Solid lines are heights in decameters where the preceeding 5 has been omitted. Dashed lines are isotachs in m/s. Plotted winds are in m/s.

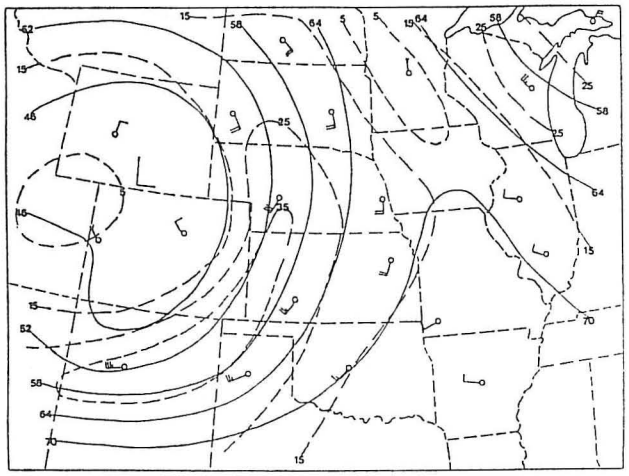

Figure 7d. 500 mb chart for 1200 GMT, 6 May 1975. Solid lines are heights in decameters where the preceding 5 has been omitted. Dashed lines are isotachs in meters per second. Plotted winds are in m/s.

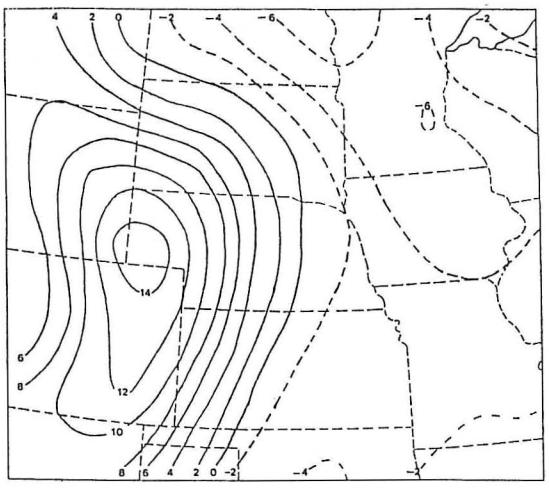

Figure 7e. Relative vorticity at 500 mb for 1200 GMT, 6 May 1975. Values are x 10^{-5} s^{-1}.

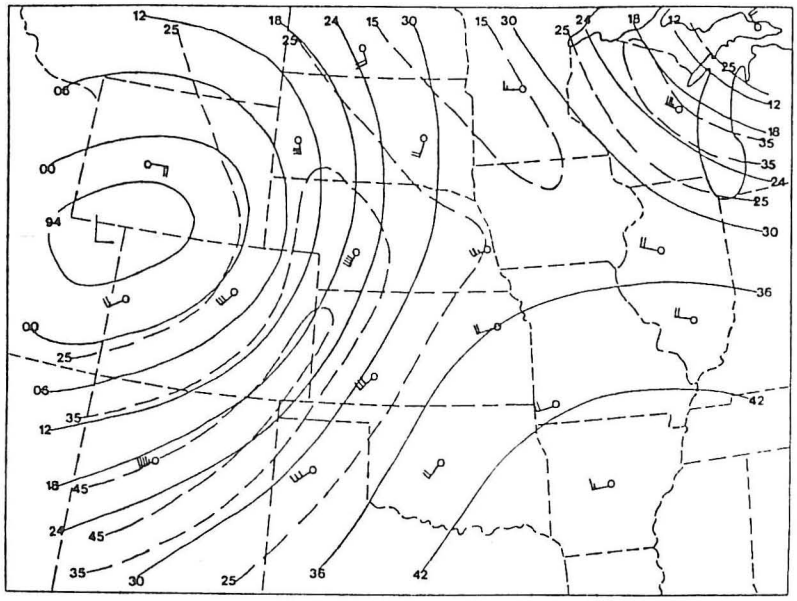

Figure 7f. 300 mb chart for 1200 GMT, 6 May 1975. Solid lines are heights in decameters where the preceeding 9 or 8 has been omitted. Dashed lines are isotachs in m/s. Plotted winds are in m/s.

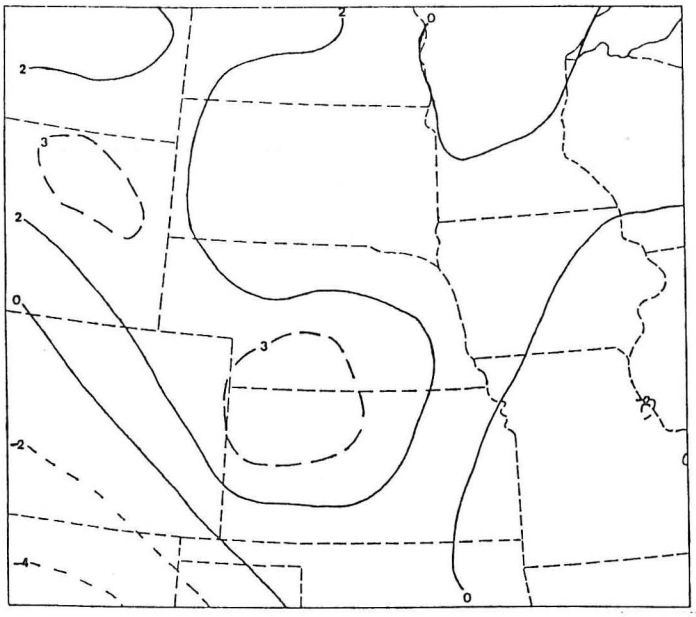

Figure 7g. Divergence at 300 mb for 1200 GMT, 6 May 1975. Values are x 10^{-5} s^{-1}.

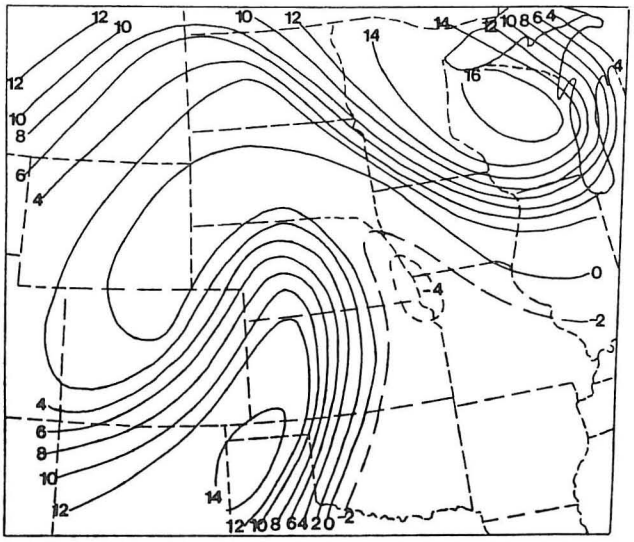

Figure 8. Lifted Index field at 1200 GMT, 6 May 1975.

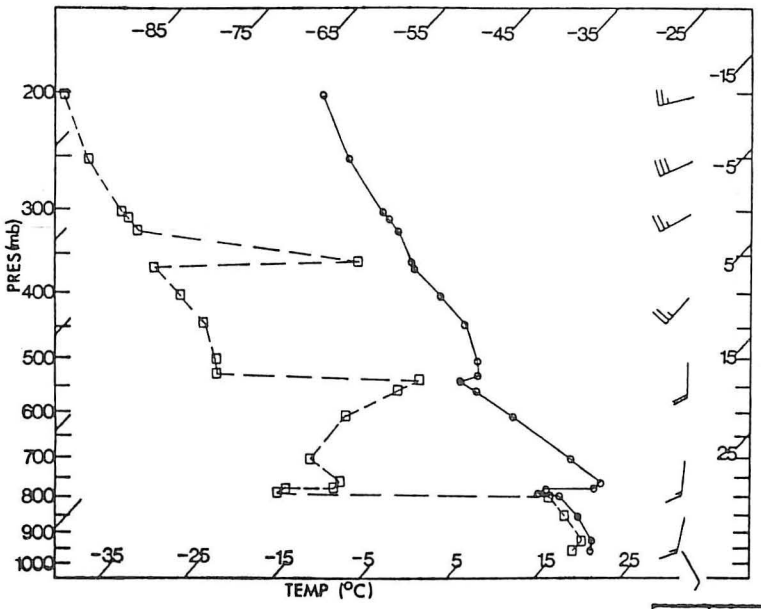

Figure 9. Sounding for Omaha, Nebraska at 1200 GMT, 6 May 1975 on Skew-T, log P diagram. Solid line is the temperature curve and dashed line is the dewpoint curve. Winds are in m/s.

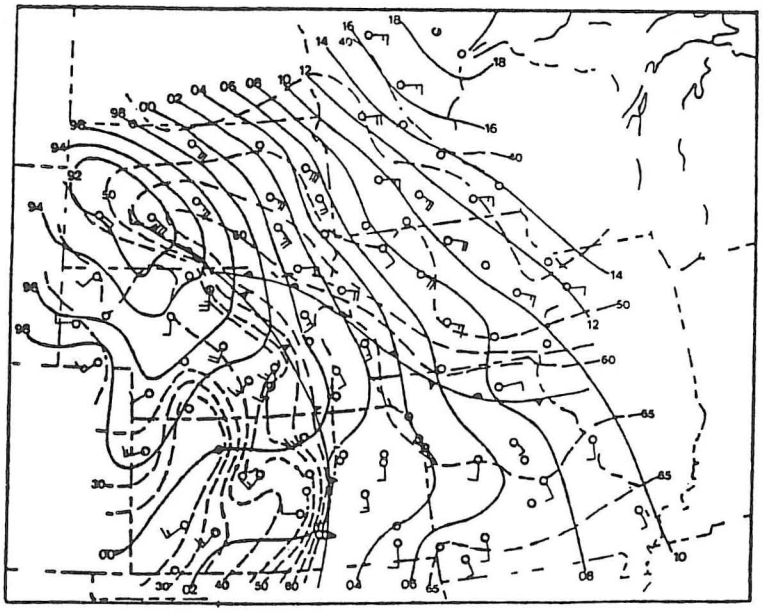

Figure 10a. Same as Figure 6a, except for 1500 GMT.

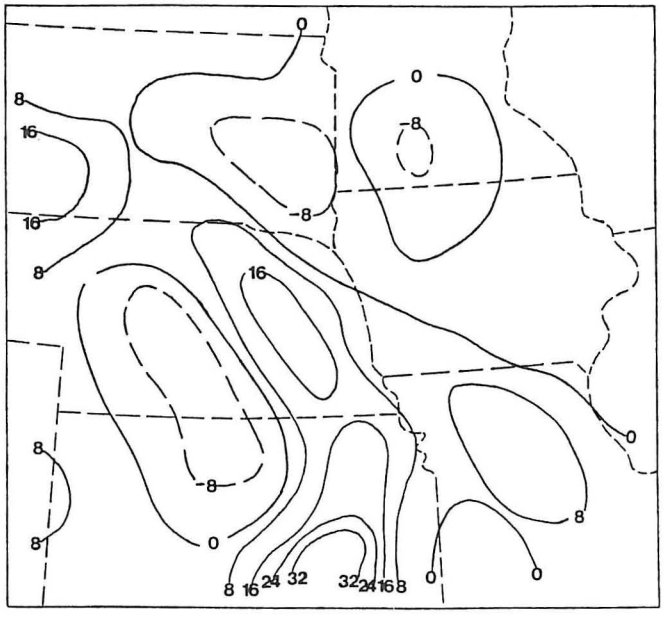

Figure 10b. Same as Figure 6b, except for 1500 GMT.

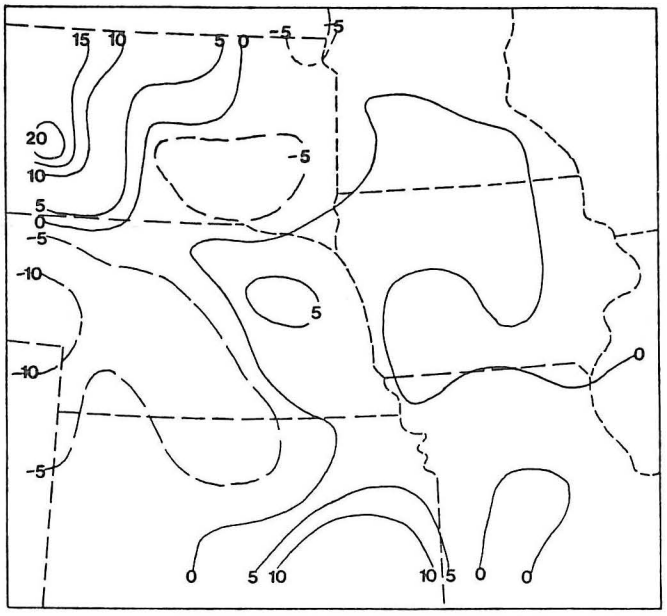

Figure 10c. Same as Figure 6c, except for 1500 GMT.

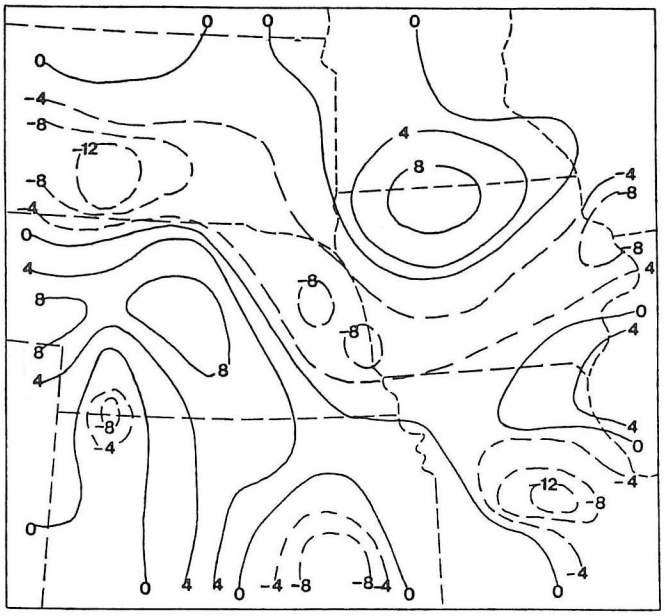

Figure 10d. Surface isallobaric divergence for 1200-1500 GMT, 6 May 1975. Values are x 10^{-5} s^{-1}.

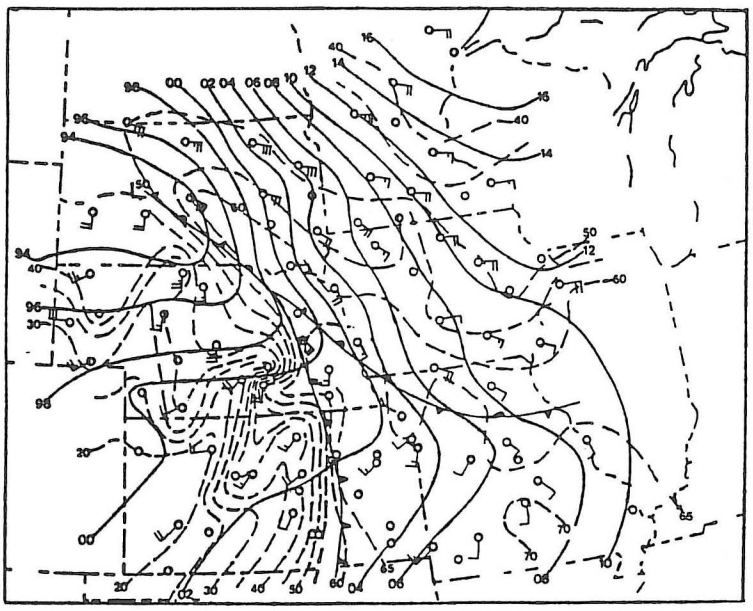

Figure 11a. Same as Figure 6a, except for 1800 GMT.

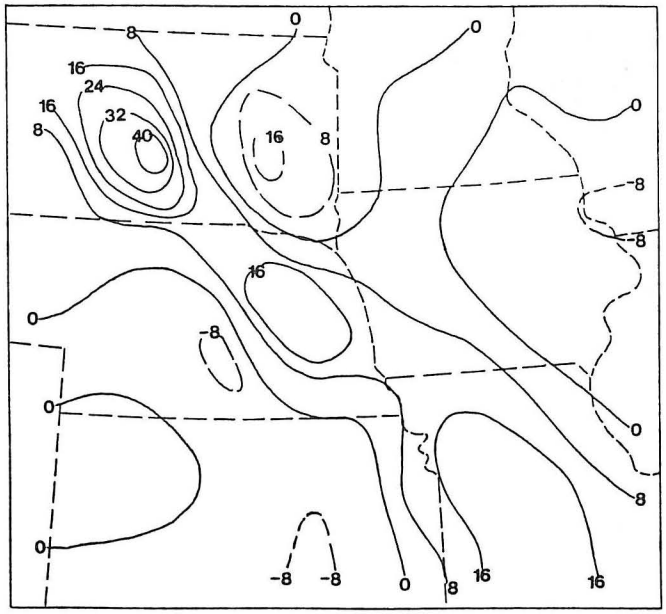

Figure 11b. Same as Figure 6b, except for 1800 GMT.

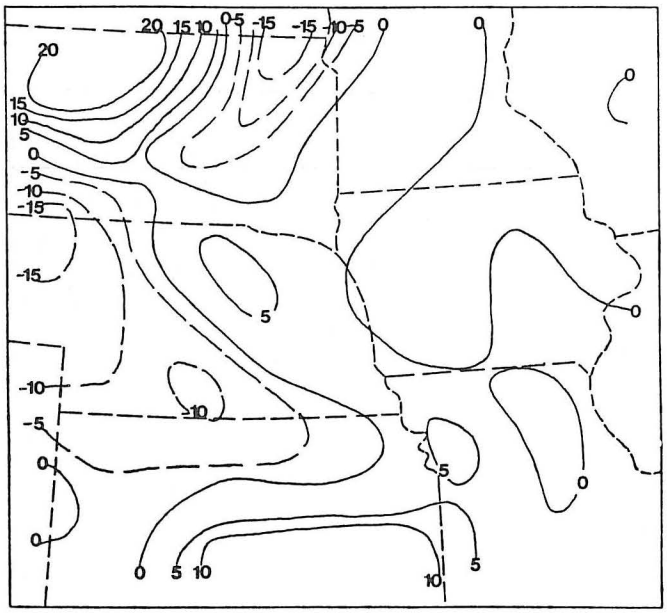

Figure 11c. Same As Figure 6c, except for 1800 GMT.

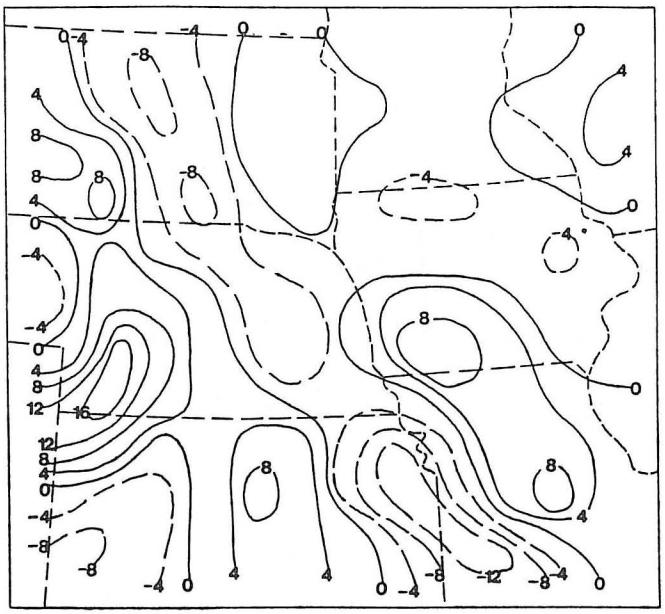

Figure 11d. Same as Figure 10d, except for 1500-1800 GMT.

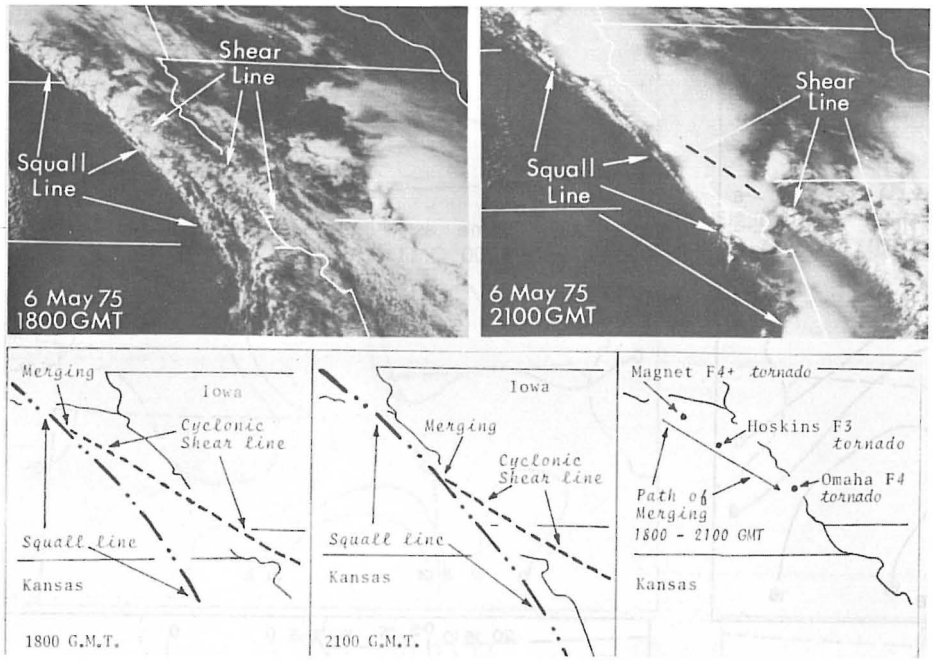

Figure 12.

Visible satellite imagery for 1800 and 1200 GMT. Note that the "shear line" is the warm frontal boundary described in the text.

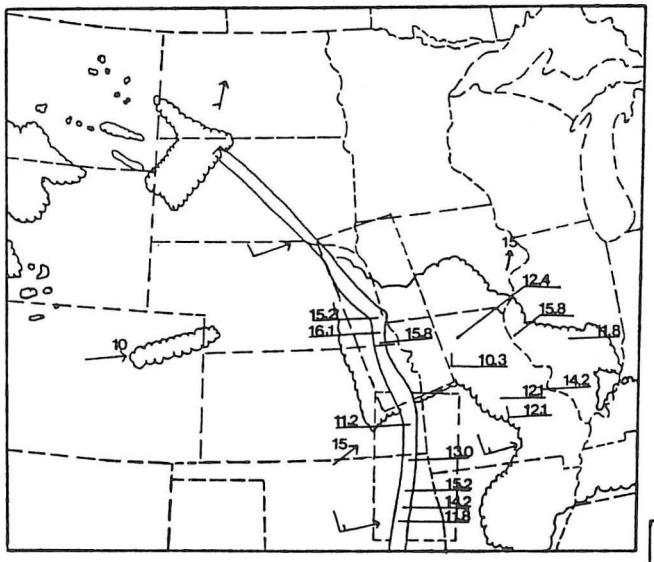

Figure 13. National Weather Service radar summary for 1935 GMT, 6 May 1975. Heights are given in kilometers. Cell movement (in m/s) is given by arrows and area movement (in m/s) is given by barbs.

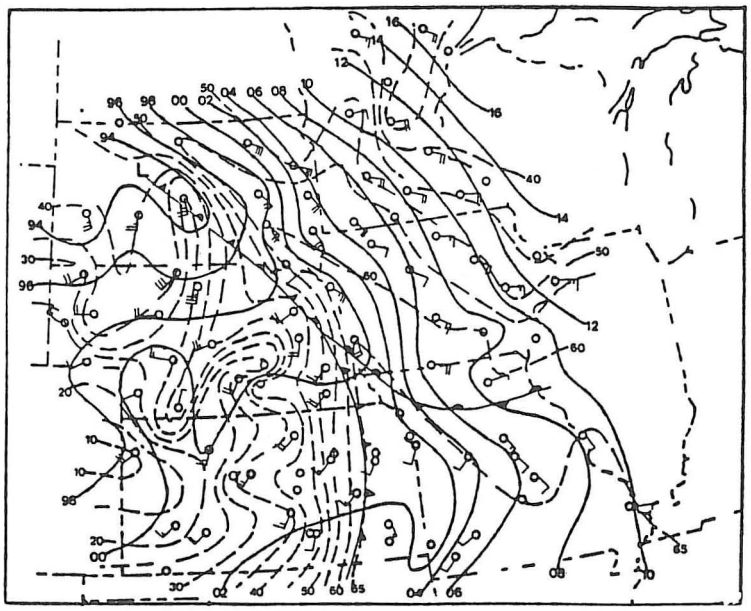

Figure 14a. Same as Figure 6a, except for 2100 GMT.

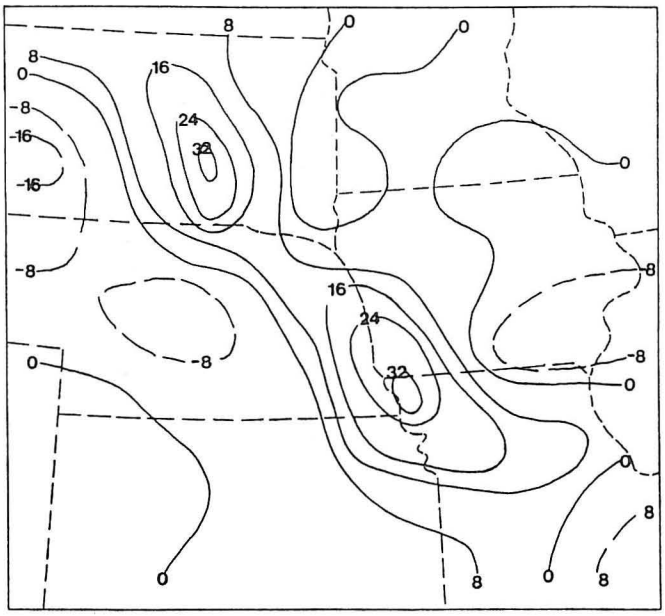

Figure 14b. Same as Figure 6b, except for 2100 GMT.

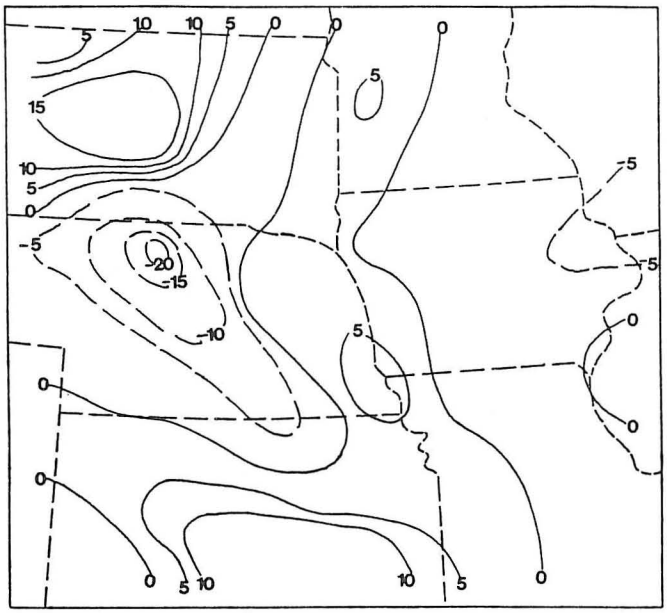

Figure 14c. Same as Figure 6c, except for 2100 GMT.

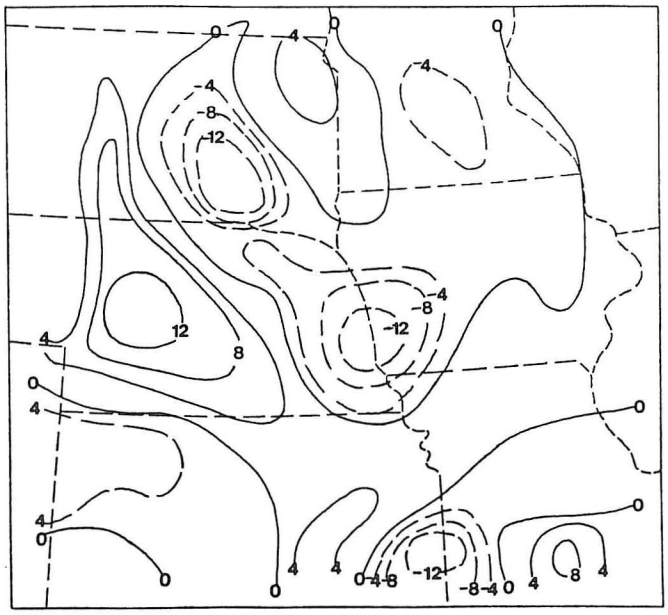

Figure 14d. Same as Figure 10d, except for 1800-2100 GMT.

FOOTNOTES AND REFERENCES

1. Dr. James T. Moore is an assistant professor of meteorology at Saint Louis University. He teaches dynamic meteorology, weather forecasting and analysis, severe storm prediction and air pollution meteorology. He is currently working on an NSF grant to investigate the use of isentropic meteorology in the short term forecasting of severe storms.

2. Mr. Harold Elkins is a second lieutenant in the United States Air Force and is presently stationed at Barksdale AFB, Louisiana. He graduated with a B.S. degree from Saint Louis University in May, 1980. He presently is an air weather briefer and forecaster for the Air Force and enjoys the challenge of forecasting severe local storms.

3. Fujita, T. T., 1973: Tornadoes Around the World. Weatherwise, 26, 56-62. 78-83.

4. Storm Data, 1975: NOAA Environmental Data Series, Asheville, N.C., 17, May.

5. Miller, J. A., 1976: An Example of Dry Line Convective Development - "The Omaha Tornado". NWS/NESS Satellite Applications Note 76/12, 4 p. [Available from Satellite Field Service Station, Federal Bldg., 601 E. 12th Street, Kansas City, MO 64106.]

6. Schaefer, J., 1974: The Life Cycle of the Dryline. J. Appl. Meteorol., 13, 444-449.

7. Rhea, J. O., 1966: A Study of Thunderstorm Formation Along Dry Lines. J. Appl. Meteorol., 5, 58-63.

8. Purdom, J., 1983: Diagnosing the Mesoscale State of the Atmosphere Using Satellite Data. Preprints, Thirteenth Conference Severe Local Storms, (Tulsa), AMS, Boston, 167-170.

9. Whiting, R. M., 1957: The Surface Chart as an Aid to Tornado Forecasting. Bull. Amer. Meteorol. Soc., 38, 353-356.

10. Miller, R. C., 1972: Notes on analysis and Severe Thunderstorm Forecasting Procedures of the Air Force Global Weather Central. Tech. Report 200 (REV). [Available from Air Weather Service/CSEF, Scott AFB, IL 62225.]

11. Kuhn, P. M., G. L. Darkow, V. E. Suomi, 1958: A Mesoscale Investigation of Pre-Tornado Thermal Environments. Bull. Amer. Meteor. Soc., 39, 224-228.

12. Karkow, G. L., V. E. Suomi and P. M. Kuhn: Surface Thermal Patterns as a Tornado Forecast Aid. Bull. Amer. Meteor. Soc., 39, 532-537.

13. Moller, A., 1980: Mesoscale Surface Analysis of the 10 April 1979 Tornadoes in Texas and Oklahoma. Preprints, Eighth Conf. on Wea. Forecasting and Anal., (Denver), AMS, Boston, 36-43.

14. Hudson, H. R., 1971: On the Relationship between Horizontal Moisture Convergence and Convective Cloud Formation. J. Appl. Meteorol., 10, 755-762.

15. Newman, W. R., 1972: The Relationship between Horizontal Moisture Convergence and Severe Storm Occurrences. M. S. Thesis, Univ. Of Oklahoma, Norman, OK, 54 pp. [Available from Univ. of Oklahoma, Norman, OK, 73019.]

16. Doswell, C. A., 1982: The Operational Meteorology of Convective Weather Volume I: Operational Mesoanalysis. NOAA Tech. Mem. NWS NSSFC-5. [Available from NSSFC, Room 1728 Federal Bldg., 601 E. 12th Street, Kansas City, MO 64106.]

17. Moore, J. T., and J. M. Murray, 1982: The Contribution of Surface, Horizontal Moisture Convergence to the Severe Convection of 10-11 April 1979. Nat. Wea. Dig., 7, 15-23.

18. Moore, J. T. and H. E. Fuelberg, 1981: A Synoptic Analysis of the First AVE-SESAME '79 Period. Bull. Amer. Meteor. Soc., 11, 1577-1590.

19. Carlson, T. N., S. G. Benjamin, G. S. Forbes and Y. F. Lin, 1983: Elevated Mixed Layers in the Regional Severe Storm Environment: Conceptual Model and Case Studies. Mon. Wea. Rev., 111, 1453-1473.

20. Beebe, F. C., and F. C. Bates, 1955: A Mechanism for Assisting in the Release of Convective Instability. Mon. Wea. Rev., 83, 1-10.

21. House, D. C., 1958: Air Mass Modification and Upper Level Divergence. Bull. Amer. Meteor. Soc., 39, 137-143.

22. McNulty, R. P., 1978: On Upper Tropospheric Kinematics and Severe Weather Occurrence. Mon. Wea. Rev., 106, 662-672.

23. Barnes, S. L., 1964: A Technique for Maximizing Details in Numerical Map Analysis. J. Appl. Meteorol., 3, 396-409.

24. Orlanski, I., 1975: A Rational Subdivision of Scales for Atmospheric Processes. Bull. Amer. Meteorol. Soc., 56, 527-530.

25. Schaefer, J., 1975: Nonlinear Biconstituent Diffusion: A Possible Trigger of Convection. J. Atmos. Sci., 32, 2278-2284.

26. Holton, J. R., 1979: An Introduction to Dynamic Meteorology, 2nd ed. Academic Press, New York, N.Y. 391 pp.

27. Tegtmeier, S. A., 1974: The Role of the Surface Subsynoptic Low Pressure System in Severe Weather Forecasting, M. S. Thesis, Univ. of Oklahoma, Norman, 66 pp. [Available from Univ. of Oklahoma, Norman, OK 73019.]